Published in final edited form as:
Dent Mater. 2012 May ; 28(5): 561–572. doi:10.1016/j.dental.2012.01.005.

Antibacterial amorphous calcium phosphate nanocomposites with a quaternary ammonium dimethacrylate and silver nanoparticles

Lei Cheng[1,2], **Michael D. Weir**[1], **Hockin H. K. Xu**[1,3,4], **Joseph M. Antonucci**[5], **Alison M. Kraigsley**[5], **Nancy J. Lin**[5], **Sheng Lin-Gibson**[5], and **Xuedong Zhou**[2]

[1]Biomaterials & Tissue Engineering Division, Dept. of Endodontics, Prosthodontics and Operative Dentistry, University of Maryland Dental School, Baltimore, MD 21201, USA

[2]State Key Laboratory of Oral Diseases, West China College of Stomatology Sichuan University, Chengdu, China

[3]Center for Stem Cell Biology & Regenerative Medicine, University of Maryland School of Medicine, Baltimore, MD 21201, USA

[4]Department of Mechanical Engineering, University of Maryland, Baltimore County, MD 21250

[5]Biomaterials Group, Polymers Division, National Institute of Standards & Technology, Gaithersburg, MD 20899, USA

Abstract

Objectives—Calcium and phosphate ion-releasing resin composites are promising for remineralization. However, there has been no report on incorporating antibacterial agents to these composites. The objective of this study was to develop antibacterial and mechanically-strong nanocomposites incorporating a quaternary ammonium dimethacrylate (QADM), nanoparticles of silver (NAg), and nanoparticles of amorphous calcium phosphate (NACP).

Methods—The QADM, bis(2-methacryloyloxyethyl) dimethylammonium bromide (ionic dimethacrylate-1), was synthesized from 2-(*N*,*N*-dimethylamino)ethyl methacrylate and 2-bromoethyl methacrylate. Ng was synthesized by dissolving Ag 2-ethylhexanoate salt in 2-(tertbutylamino)ethyl methacrylate. Mechanical properties were measured in three-point flexure with bars of 2×2×25 mm (n = 6). Composite disks (diameter = 9 mm, thickness = 2 mm) were inoculated with *Streptococcus mutans*. The metabolic activity and lactic acid production of biofilms were measured (n = 6). Two commercial composites were used as controls.

Results—Flexural strength and elastic modulus of NACP+QADM, NACP+NAg, and NACP +QADM+NAg matched those of commercial composites with no antibacterial property ($p > 0.1$).

Correspondence: Dr. Hockin H. K. Xu, Professor, Director of Biomaterials & Tissue Engineering Division, Department of Endodontics, University of Maryland Dental School, Baltimore, MD 21201 (hxu@umaryland.edu). Dr. Xuedong Zhou, Professor, Dean, West China College of Stomatology, Sichuan University, China (zhouxd@scu.edu.cn)..

The NACP+QADM+NAg composite decreased the titer counts of adherent *S. mutans* biofilms by an order of magnitude, compared to the commercial composites ($p < 0.05$). The metabolic activity and lactic acid production of biofilms on NACP+QADM+NAg composite were much less than those on commercial composites ($p < 0.05$). Combining QADM and NAg rendered the nanocomposite more strongly antibacterial than either agent alone ($p < 0.05$).

Significance—QADM and NAg were incorporated into calcium phosphate composite for the first time. NACP+QADM+NAg was strongly-antibacterial and greatly reduced the titer counts, metabolic activity, and acid production of *S. mutans* biofilms, while possessing mechanical properties similar to commercial composites. These nanocomposites are promising to have the double benefits of remineralization and antibacterial capabilities to inhibit dental caries.

Keywords

Antibacterial nanocomposite; amorphous calcium phosphate; quaternary ammonium salt; silver nanoparticles; *Streptococcus mutans* biofilm; stress-bearing; tooth caries inhibition

1. Introduction

Approximately half of all dental restorations fail within 10 years, and replacing them consumes nearly 60% of the average dentist's practice time [1–4]. Dental composites are increasingly used due to their excellent esthetics and improved performance [5–11]. However, composites *in vivo* had more biofilm and plaque accumulation than other restorative materials [12–15]. Plaques adjacent to the restoration margins could result in secondary caries and compromise the restoration's longevity. Indeed, previous reports demonstrated that: (1) the two main challenges facing composite restorations are secondary caries and bulk fracture [16,17]; (2) caries at the restoration margins are a main reason for replacing the existing restorations [1]; (3) replacing the failed restorations accounts for 50–70% of all restorations [2,3]; (4) replacement dentistry costs $5 billion in the USA each year [18]. Therefore, there is a great need to improve the longevity of composite restorations by incorporating bioactive agents to combat microbial destruction and recurrent caries while sustaining the load-bearing capability [4].

Acidogenic bacteria such as *Streptococcus mutans* (*S. mutans*) and their biofilms, upon exposure to fermentable carbohydrates, are responsible for dental caries [19–23]. Hence, efforts have been made to develop antibacterial dental composites. One important class of such composites involved the use of polymers containing quaternary ammonium salts (QAS) [24–28]. QAS are widely used in water treatment, surface coatings, and the food industry due to their low toxicity and potent antimicrobial activity [29]. Antibacterial QAS monomers such as 12-methacryloyloxydodecylpyridinium bromide (MDPB) [24] copolymerize with other monomers in the composite to form polymer matrices that can combat bacteria. The resulting composite decreased the attachment of *S. mutans* and plaque accumulation, and inhibited the progression of secondary root caries [30]. Recently, a unique QAS dimethacrylate monomer was synthesized and incorporated into dental polymers to effectively reduce *S. mutans* colonization [31].

A second class of antibacterial dental composites contain silver (Ag) that can kill oral bacteria such as *S. mutans* [32,33]. Ag is known to have antibacterial, antifungal, and antiviral capabilities [34,35]. For dental composites, it is desirable to incorporate silver nanoparticles with a high surface area into the resin to reduce the Ag particle concentration necessary for efficacy [36,37]. Thus, it would be possible to obtain a strong antibacterial capability without compromising the composite color and mechanical properties. Indeed, a recent study used a unique approach to prepare nanocomposites with evenly dispersed Ag

nanoparticles at a mass fraction of 0.08% to achieve a 40% reduction in bacteria coverage on the nanocomposites [38].

Another class of dental composites contains calcium phosphate (CaP) particles as a portion of the filler phase for remineralization purposes [39–42]. These composites released supersaturating levels of calcium (Ca) and phosphate (PO_4) ions and remineralized tooth lesions *in vitro* [40,42]. Recently, novel CaP nanoparticles of sizes of about 100 nm were synthesized via a spray-drying technique and filled into dental composites [41,43]. These nanocomposites achieved Ca and PO_4 release similar to those of previous CaP composites, while possessing much better mechanical properties [41,43]. A literature search revealed no report on combining the best of the three therapeutic approaches: antibacterial monomers, antibacterial Ag nanoparticles, and Ca and PO_4 ion release via CaP nanoparticles. The rationale for this combination was for the composites to not only have a remineralization capability as previous studies have demonstrated, but also to possess strong antibacterial activities.

Therefore, the objective of the present study was to develop novel nanocomposites with ACP and Ag nanoparticles in a QAS-containing resin matrix to achieve caries-inhibiting and stress-bearing capabilities. It was hypothesized that (1) adding QAS or Ag nanoparticles to the ACP nanocomposite would result in significant antibacterial properties; (2) adding QAS and Ag together in the same nanocomposite would achieve even stronger antibacterial capabilities; (3) the novel antibacterial nanocomposites would have mechanical properties matching those of commercial composites without antibacterial capabilities.

2. Materials and methods

2.1 Fabrication of calcium phosphate nanocomposite

A spray-drying technique as described previously [41,44] was used to make nanoparticles of ACP ($Ca_3[PO_4]_2$). To make nanoparticles of ACP (referred to as NACP), calcium carbonate ($CaCO_3$, Fisher, Fair Lawn, NJ) and dicalcium phosphate anhydrous ($CaHPO_4$, Baker Chemical Co., Phillipsburg, NJ) were dissolved into an acetic acid solution to obtain final Ca and PO_4 ionic concentrations of 8 mmol/L and 5.333 mmol/L, respectively. This resulted in a Ca/P molar ratio of 1.5, the same as that for ACP. This solution was sprayed into a heated chamber, and an electrostatic precipitator (AirQuality, Minneapolis, MN) was used to collect the dried particles. This produced NACP with a mean particle size of 116 nm, as measured in a previous study [45].

Two types of co-fillers were used for reinforcement: barium boroaluminosilicate glass particles of a mean diameter of 1.4 μm (Caulk/Dentsply, Milford, DE), and nano-sized silica glass (Aerosil-OX50, Degussa, Ridgefield, NJ) with a mean diameter of 40 nm. Each glass was silanized with 4% 3-methacryloxypropyltrimethoxysilane and 2% n-propylamine (all by mass, unless otherwise noted). A resin of BisGMA (bisphenol glycerolate dimethacrylate) and TEGDMA (triethylene glycol dimethacrylate) at 1:1 mass ratio was rendered light-curable with 0.2% camphorquinone and 0.8% ethyl 4-N,N-dimethylaminobenzoate (referred to as BisGMATEGDMA resin). The NACP mass fraction in the resin was 30%, and the glass mass fraction was 35%, following a previous study [45]. The resin filled with 30% NACP without any glass fillers is referred to as “Resin with 30% NACP without glass”. The composite filled with 30% NACP + 35% nano-silica is referred to as “NACP+nano silica composite”. The composite filled with 30% NACP + 35% barium boroaluminosilicate glass is referred to as “NACP composite”.

2.2 Fabrication of QAS and silver nanocomposites

The synthesis of bis(2-methacryloyloxyethyl) dimethylammonium bromide, termed ionic dimethacrylate-1 (IDMA-1), was described recently [31]. IDMA-1 was selected as the quaternary ammonium dimethacrylate (QADM) to incorporate into the nanocomposites in the present study. Its synthesis was carried out using a modified Menschutkin reaction, where a tertiary amine group was reacted with an organo-halide. A benefit of this reaction is that the reaction products are generated at virtually quantitative amounts and require minimal purification [31]. Briefly, 10 mmol of 2-(*N*,*N*-dimethylamino)ethyl methacrylate (DMAEMA, Sigma-Aldrich, St. Louis, MO) and 10 mmol of 2-bromoethyl methacrylate (BEMA, Monomer-Polymer and Dajec Labs, Trevose, PA) were combined with 3 g of ethanol in a 20 mL scintillation vial. A magnetic stir bar was added, and the vial was stirred at 60 °C for 24 h. The solvent was removed via evaporation, forming a clear, colorless, and viscous liquid. The QADM thus obtained was then mixed with the photo-activated BisGMA-TEGDMA resin at a QADM mass fraction of 20%. This resin is referred to as the BisGMA-TEGDMA-QADM resin. A previous study showed that 20% QADM greatly reduced bacterial growth on the polymer surfaces [31]. The BisGMA-TEGDMA-QADM resin was then filled with 30% NACP and 35% barium boroaluminosilicate glass, and this composite is referred to as “NACP+QADM”. Hence, the QADM mass fraction in the final composite was 20% × 35% = 7%.

Silver 2-ethylhexanoate powder (Strem Chemicals, New Buryport, MA) at 0.08 g was dissolved into 1 g of 2-(tert-butylamino)ethyl methacrylate (TBAEMA, Sigma) by stirring, and then 1% of this solution was added to the resin. The mass fraction of Ag salt in the resin was 0.08%, according to a recent study [38]. TBAEMA improves the solubility by forming Ag-N coordination bonds with Ag ions, thereby facilitating the Ag salt to dissolve in the resin solution. TBAEMA was specifically selected since it contains reactive methacrylate groups and therefore can be chemically incorporated into the polymer network upon photopolymerization [38].

To fabricate the “NACP+NAg” composite, the Ag-TBAEMA was mixed with BisGMA-TEGDMA, and then 30% NACP and 35% barium boroaluminosilicate glass were added to the resin. Since the resin mass fraction was 35% in the composite, the 0.08% of Ag in the resin yielded 0.028% of Ag mass fraction in the composite. To fabricate the “NACP +QADM+NAg” composite, the Ag-TBAEMA was mixed with the BisGMA-TEGDMA-QADM resin. NACP and glass filler levels were selected to yield a cohesive paste that was readily mixed and not dry [45]. Each paste was placed into rectangular molds of (2 × 2 × 25) mm for mechanical testing, and disk molds of 9 mm in diameter and 2 mm in thickness for biofilm experiments. The specimens were photo-polymerized (Triad 2000, Dentsply, York, PA) for 1 min on each side.

In addition, a commercial composite with glass nanoparticles of 40 nm to 200 nm and a low level of F release was tested (Heliomolar, Ivoclar, Ontario, Canada) and is referred to as “CompositeF”. The fillers were silica and ytterbium-trifluoride with a filler level of 66.7%. Heliomolar is indicated for Class I and Class II restorations in the posterior region, Class III–V restorations, and pit and fissure sealing. Another commercial composite, Renamel (Cosmedent, Chicago, IL), served as a non-releasing control (referred to as “CompositeNoF”). It consisted of nanofillers of 20 nm to 40 nm with 60% (by mass) fillers in a multifunctional methacrylate ester resin [46]. Renamel is indicated for Class III, IV, and V restorations. The control specimens were also photo-cured in the same manner as described above.

2.3 Transmission electron microscopy (TEM)

TEM was performed to examine the silver nanoparticles in the resin. The mass fraction of the Ag salt was 0.08% in the resin, the same as that described above. Following a previous study [38], a thin sheet of mica was partially split and the Ag-containing resin was placed in the gap. The resin-mica sandwich was pressed with an applied load of 2.7×10^7 N to form a thin sheet of resin in between the two mica layers [38]. The resin in the mica was photo-cured for 1 min on each side in the same manner as described above. The mica sheet was then split apart after 1 day using a scalpel to expose the polymerized film. An ultrathin layer of carbon was vacuum-evaporated onto the composite (Electron Microscopy Sciences, Hatfield, PA). The carbon-coated sample was then partially submerged in distilled water in order to float the thin film onto the water's surface. A copper grid was then used to retrieve the film. After drying, TEM was performed on a Tecnai T12 high resolution transmission electron microscope (FEI Company, Hillsboro, OR) using an accelerating voltage of 120 kV. The TEM images were collected and the sizes of the silver particles were measured using AMT V600 image analysis software (Advanced Microscopy Techniques, Woburn, MA).

2.4 Flexural testing

The composite bars were immersed in distilled water at 37 °C for 1 day. Hydrated specimens were then fractured in three-point flexure with a 10-mm span at a crosshead-speed of 1 mm/min on a computer-controlled Universal Testing Machine (5500R, MTS, Cary, NC). Flexural strength (S) was calculated as: $S = 3P_{max}L/(2bh^2)$, where P_{max} is the fracture load, L is span, b is specimen width and h is specimen thickness. Elastic modulus (E) was calculated as: $E = (P/d)(L^3/[4bh^3])$, where load P divided by displacement d is the slope of the load-displacement curve in the linear elastic region. The specimens were fractured while still wet, within several minutes from being taken out of water. Six specimens were tested for each material (n = 6).

2.5 S. mutans inoculation and live/dead assay

S. mutans was selected because it is a cariogenic bacterium and is the primary causative agent of dental caries [19]. *S. mutans* bacteria were obtained commercially (ATCC 700610, UA159, American Type Culture, Manassas, VA). Their use was approved by University of Maryland. The growth medium consisted of brain heart infusion (BHI) broth (BD, Franklin Lakes, NJ) supplemented with 0.2 % sucrose. Fifteen μL of stock bacteria was added to 15 mL of growth medium and incubated at 37 °C with 5 % CO_2 for 16 h, during which the *S. mutans* were suspended in the growth medium. The inoculation medium was formed by diluting this *S. mutans* culture 10-fold in growth medium [47].

Six composites were tested in biofilm experiments: The four nanocomposites listed in Table 1, and the two control composites. Composite disks were sterilized in an ethylene oxide sterilizer (Anprolene AN 74i, Andersen, Haw River, NC). For each composite, six disks (n = 6) were used for each biofilm experiment at each time point, except for live/dead staining in which three disks were used for each composite at each time point. Each disk was placed in a well of a 24-well plate and inoculated with 1.5 mL of inoculation medium. The samples were incubated at 5% CO_2 and 37 °C for 1 d to form the initial biofilms, or 3 d to form mature biofilms. The growth medium was changed every 24 h, by transferring the disks to a new 24-well plate with fresh medium. After 1 or 3 d, the biofilms on the disks were washed three times with phosphate buffered saline (PBS) to remove loose bacteria, and then stained using the BacLight live/dead kit (Molecular Probes, Eugene, OR). Live bacteria were stained with Syto 9 to produce green fluorescence, and bacteria with compromised membranes were stained with propidium iodide to produce red fluorescence. The stained disks were examined using an inverted epifluorescence microscope (Eclipse TE2000-S,

Nikon, Melville, NY). At each time period, four images were collected on each of three disks per material, yielding 12 images for each condition.

2.6 MTT metabolic assay

The composite disks were placed in a 24-well plate, inoculated with 1.5 mL of the inoculation medium, and cultured for 1 d or 3 d. Each disk was transferred to a new 24-well plate for the MTT (3-(4,5-Dimethylthiazol-2-yl)-2,5-diphenyltetrazolium bromide) assay. It is a colorimetric assay that measures the enzymatic reduction of MTT, a yellow tetrazole, to formazan. The MTT assay for *S. mutans* biofilms was previously described [48]. Briefly, 1 mL of MTT dye (0.5 mg/mL MTT in PBS) was added to each well and incubated at 37 °C in 5% CO_2 for 1 h. During this process, metabolically active bacteria reduced the MTT to purple formazan. After 1 h, the disks were transferred to a new 24-well plate, 1 mL of dimethyl sulfoxide (DMSO) was added to solubilize the formazan crystals, and the plate was incubated for 20 min with gentle mixing at room temperature in the dark. After brief mixing via pipetting, 200 μL of the DMSO solution from each well was transferred to a 96-well plate, and the absorbance at 540 nm (optical density OD_{540}) was measured via a microplate reader (SpectraMax M5, Molecular Devices, Sunnvale, CA). A higher absorbance indicates a higher formazan concentration, which in turn indicates more metabolic activity in the biofilm on the composite.

2.7 Lactic acid production and viable cell counts

Composite disks with 3 d biofilms were rinsed in cysteine peptone water (CPW) to remove loose bacteria. Each disk was placed in a new 24-well plate and 1.5 mL of buffered peptone water (BPW) supplemented with 0.2% sucrose was added. BPW medium was used so that the mature biofilm would remain stable during the 3 h acid production assay. The relatively high buffer capacity of BPW should prevent the pH from becoming significantly acidic, as a low pH would hinder bacterial acid production. Disks with biofilms were incubated at 5% CO_2 and 37 °C for 3 h to allow the biofilms to produce acid. After 3 h, the BPW solutions were stored for lactate analysis. Lactate concentrations in the BPW solutions were determined using an enzymatic (lactate dehydrogenase) method [49]. The microplate reader was used to measure the absorbance at 340 nm (OD_{340}) for the collected BPW solutions. Standard curves were prepared using a lactic acid standard (Supelco Analytical, Bellefonte, PA).

After the disks with biofilms were treated for lactic acid production, colony-forming unit (CFU) counts were used to quantify the total number of viable bacteria present on each composite disk. When biofilms are properly dispersed and diluted, each viable bacterium results in a single, countable colony on an agar plate. The disks were transferred into tubes with 2 mL CPW. The biofilms were harvested by sonicating (3510R-MTH, Branson, Danbury, CT) for 3 min, and then vortexing at maximum speed for 20 s using a vortex mixer (Fisher, Pittsburgh, PA). This protocol removed and dispersed the biofilms from the disks. The bacterial suspensions were serially diluted, spread onto BHI agar plates, and incubated for 3 d at 5% CO_2 and 37 °C. At 1 d and 3 d, the number of colonies that grew were counted and used, along with the dilution factor, to calculate total CFUs on each disk.

2.8 Statistical analysis

One-way and two-way analyses of variance (ANOVA) were performed to detect the significant effects of the variables. Tukey's multiple comparison test was used to compare the data at a p-value of 0.05. Each standard deviation (sd) serves as the estimate for the standard uncertainty associated with a particular measurement.

3. Results

Typical TEM micrographs of the Ag nanoparticles in the resin are shown in Fig. 1: (A) Ag nanoparticles at a lower magnification (A), and at a high magnification (B). The Ag particle size was measured for 100 random particles to be (2.7 ± 0.6) nm. The particles appeared to be well dispersed in the resin, without noticeable clustered particles or significant agglomerates.

Mechanical properties are plotted in Fig. 2 for (A) flexural strength, and (B) elastic modulus (mean ± sd; n = 6). In (A), the resin with 30% NACP without glass had a slightly lower flexural strength. Bars with dissimilar letters indicate values that are significantly different ($p < 0.05$). The NACP composite had a strength of (62 ± 8) MPa, not significantly different from the (57 ± 12) MPa of CompositeF, and (56 ± 9) MPa of CompositeNoF ($p > 0.1$). Adding QADM, NAg, or QADM+NAg yielded strengths of (53 ± 7) MPa, (67 ± 6) MPa and (54 ± 12) MPa, respectively ($p > 0.1$). In (B), the resin with 30% NACP without glass had the lowest elastic modulus ($p < 0.05$). The NACP composite, which contained 35% barium glass, had a higher elastic modulus ($p < 0.05$). The NACP+nano silica composite had a modulus similar to those of the commercial control composites ($p > 0.1$).

Fig. 3 shows typical live/dead staining photos of biofilms on composites at 1 d. Live bacteria were stained green, and the compromised bacteria were stained red. When the live and dead bacteria were in close proximity, the biofilm was co-stained with the two fluorophores, resulting in yellowish or orange colors. The biofilms on CompositeNoF, CompositeF, and NACP composite were predominantly viable, with small amounts of dead cells. There was a slight increase in the amount of dead cells on NACP+QADM, as indicated by the arrow in (D). There was noticeably less green staining, and more red/orange staining, in the biofilms on NACP+NAg composite (arrows in E). The numbers of dead bacteria, indicated by red/orange staining, further increased in the biofilms on NACP+QADM+NAg composite (arrows in F).

The 3 d live/dead biofilm images are shown in Fig. 4. On CompositeNoF, CompositeF, and NACP composite, *S. mutans* had formed mature biofilms in which the staining was mostly green, indicating that the bacteria were primarily alive. NACP+QADM had slightly more dead bacteria (arrow in D). The amount of compromised bacteria significantly increased in (E) on NACP+NAg composite. Visual examination revealed that the NACP+QADM+NAg composite had the most red/orange staining, indicating the most compromised bacteria.

Fig. 5 plots the biofilm metabolic activity measured via the MTT assay at (A) 1 d, and (B) 3 d. At both 1 d and 3 d, CompositeNoF had the highest MTT absorbance, indicating the highest metabolic activity in the biofilms adherent on the composite disks. The incorporation of QADM and NAg into the NACP composite significantly decreased the metabolic activity of the *S. mutans* biofilms ($p < 0.05$). Furthermore, incorporating QADM and NAg together into the same composite resulted in the lowest metabolic activity ($p < 0.05$).

Fig. 6 plots the CFU counts. At 1 d, the CFU counts were 27 million per disk for CompositeNoF and 21 million for NACP composite. The CFU counts were greatly reduced to 12.5 million on NACP+QADM composite, 3.2 million on NACP+NAg composite, and 1.4 million on NACP+QADM+NAg composite ($p < 0.05$). The ranking of CFU at 1 d is maintained at 3 d, with the NACP+QADM+NAg composite having the least CFU counts, which were an order of magnitude less than that of CompositeNoF.

Fig. 7 plots the lactic acid production by biofilms on composites. The biofilms on CompositeNoF produced the most acid, followed by that of CompositeF and NACP composite. The incorporation of either QADM or NAg into the NACP composite

significantly decreased the acid production ($p < 0.05$). When both QADM and NAg were incorporated, the composite resulted in the lowest acid production by the biofilms ($p < 0.05$). The biofilm acid production on NACP+QADM+NAg composite was nearly 1/3 that on CompositeNoF.

4. Discussion

So far there have been no reports on the incorporation of quaternary ammonium salts and silver nanoparticles into resin-based calcium phosphate dental composites. In the present study, NAg and QADM were incorporated into ACP nanocomposite for the first time. The NACP+QADM+NAg composite greatly reduced the *S. mutans* biofilm growth, metabolic activity, CFU counts, and lactic acid production, compared to two commercial composites. In addition, NACP+QADM+NAg possessed mechanical properties similar to the commercial composites. In the oral environment, bacteria colonize on the tooth-restoration surface to form a biofilm, which is a heterogeneous structure consisting of clusters of various types of bacteria embedded in an extracellular matrix [50]. Cariogenic bacteria such as *S. mutans* and lactobacilli in the plaque metabolize carbohydrates to acids, causing demineralization of the tooth structure and the tooth-restoration margins beneath the biofilm. Therefore, this new nanocomposite exhibits a great reduction in *S. mutans* biofilm growth and acid production and suggests a promising approach to combat recurrent caries.

The present study showed that biofilms on the composite with no F release had the highest metabolic activity, CFU counts, and acid production of the materials tested. These results are consistent with previous studies that showed that, in general, resin composites had no antimicrobial capability and accumulated more biofilms and plaque *in vitro* and *in vivo* compared to other restorative materials [12,14,15]. The present study showed that the composite with F release (CompositeF) slightly reduced the biofilm growth, yielding lower CFU counts and less acid, compared to CompositeNoF. This is also consistent with previous studies, which showed that F ions reduced the acid production of biofilms [51]. The reason for the reduction in acid production by bacteria was suggested to be the F ions inhibiting the metabolic pathways such as the fermentation pathway of the bacteria for the lactic acid production [50]. In addition, the present study showed that the NACP composite also had a slight reduction in biofilm growth and acid production, similar to that of CompositeF. It is possible that the alkalinity of the NACP may slightly reduce the bacteria growth [52]. It should be noted that another merit of the NACP composite is its release of calcium (Ca) and phosphate (PO_4) ions [45]. The amount of release was similar to those in previous studies that effectively remineralized tooth lesions *in vitro* [40,42]. The NACP was combined with antibacterial agents QADM and NAg in the present study for the first time. The purpose was to combine the best of both worlds: The remineralization capability of NACP, and the antibacterial activity of QADM and NAg.

QAS include polymerizable monomers and non-polymerizable small molecules. QAS monomers have been incorporated into dental composites with important antibacterial properties [13,24,26–28,53,54]. The advantage of QAS composites is that the antibacterial agent is copolymerized with the resin by forming a covalent bonding with the polymer network, and therefore is immobilized in the composite and not released or lost over time. This method imparts a durable and permanent antibacterial capability to the composite. For example, a study on MDPB monomer, a QAS bromide monomethacrylate, showed that the antibacterial effect was maintained after the composite was immersed in water for 3 months [13]. A QAS chloride was used to synthesize an antibacterial bonding agent [26]. QAS bromides and chlorides at different chain lengths were incorporated into a glass ionomer cement, yielding long-lasting antimicrobial capabilities [27]. In addition, QAS nanoparticles were added to a composite that was shown to be effective against *S. mutans* [54].

While MDPB [13,25] and QAS chloride [26] are both monomethacrylates, a recent study synthesized the first QAS monomers that were dimethacrylates (QADM) [31]. *S. mutans* coverage from 100% on the control to about 50% on materials containing IDMA-1 [31]. These previous findings agree with the present study, which showed that NACP composites containing the same QADM had CFU counts approximately half of those on composites without QADM. The present study used QADM because its synthetic method was fairly straightforward when compared to the synthesis of other QAS monomers. In addition, as a dimethacrylate, QADM could be beneficial when compared to QAS monomethacrylates. QADM has reactive groups on both ends of the molecule, which could be incorporated into the resin matrix with less of a negative impact on the mechanical and physical properties of the composite. In contrast, a monomethacrylate QAS has only one reactive group and may weaken the resin matrix. Furthermore, this QADM is a low viscosity monomer that is miscible with common dimethacrylates and is expected to have minimal monomer leachability, compared with other quaternary ammonium salts based on monomethacylates. The detailed antimicrobial mechanism of QAS is yet to be established; however, it appears that QAS materials can cause bacteria lysis by binding to the cell membrane and causing cytoplasmic leakage [54]. When the negatively charged bacterial cell contacts the positively charged (N^+) sites of the QAS resin, the electric balance of the cell membrane could be disturbed, and the bacterium could explode under its own osmotic pressure [55]. The present study shows that the use of this QADM in composites is effective in reducing CFU counts, metabolic activity, and acid production of *S. mutans* biofilms.

Ag is another effective and widely used antibacterial agent with a strong toxicity to a wide range of micro-organisms [36,56–58]. The antimicrobial mechanism appears to be that the Ag ions interact and inactivate the vital enzymes of bacteria, and cause the DNA in the bacteria to lose its replication ability leading to cell death [36,58]. Ag has a low toxicity and good biocompatibility with human cells [57], has a long-term antibacterial effect due to sustained silver ion release [59], and can result in less bacterial resistance than antibiotics [60]. For dental composites, silver ion-implanted silica fillers and silver-containing silica prepared by sol-gel have been evaluated as fillers [32,33]. Ag-supported silica gel in a composite inhibited *S. mutans* growth and appeared to have a long-lasting effect [33]. More recently, Ag nanoparticles were shown to be highly effective for antibacterial applications [36,58]. Novel Ag nanoparticle-containing resins were developed [37,38]. Ag 2-ethylhexanoate salt does not dissolve well in the hydrophobic BisGMA-TEGDMA monomers. Therefore, in the present study, the Ag salt was dissolved in the TBAEMA monomer, which was then mixed with the BisGMA-TEGDMA monomers. The Ag ions were thus distributed in the BisGMA-TEGMDA resin. These Ag ions agglomerated to form the nanoparticles that became part of the composite upon photopolymerization. An advantage of this method was that it reduced the Ag salt to the Ag nanoparticles in the resin, avoiding the challenge of mixing preformed Ag nanoparticles that could form large agglomerates. Another advantage was that the TBAEMA used to dissolve the Ag salt contained a reactive methacrylate functionality, and hence it could be chemically incorporated into the polymer network upon photopolymerization. The TEM examination showed that the Ag nanoparticles thus formed were about 2.7 nm in diameter, and the particles were well dispersed in the resin with no noticeable areas of excessive particle aggregation. Adding Ag nanoparticles to the composite greatly increased its antibacterial capability. The CFU counts on the NACP+NAg composite were less than one third that of the counts on NACP composite. MTT and lactic acid production on the NACP+NAg composite were also significantly less than that on NACP composite. Therefore, the concurrent reduction of Ag ions and polymerization of dimethacrylate-based polymers is a promising method to incorporate Ag nanoparticles and impart a potent antibacterial capability to the ACP nanocomposite.

Previous studies either used QAS or NAg in dental materials. So far there have been no reports on the use of QAS and NAg together in the same composite. In the present study, visual examination of the live/dead images indicated that the composite with QADM and NAg had the least amount of live bacteria (green staining) and the most amount of compromised bacteria (yellow/orange staining). Quantitative measurements showed that the incorporation of both QADM and NAg together in the same composite significantly lowered the CFU counts, metabolic activity, and lactic acid production, compared to separately adding either the QADM or Ag nanoparticles. Biofilms on the NACP+QADM+NAg composite had the lowest CFU count, metabolic activity, and acid production of all the biofilms. Therefore, this study shows that it is beneficial to use multiple agents (QADM + NAg) rather than a single agent. Among the three antibacterial nanocomposites, NACP +QADM+NAg is advantageous because it has the strongest antibacterial effects, while being mechanically as strong as the other composites. Regarding the long-term durability of the antibacterial effects, previous studies showed that the quaternary ammonium methacrylate was co-polymerized with the resin composite and therefore had a long-lasting antibacterial activity [24,25]. Other studies showed that Ag-containing composite inhibited *S. mutans* growth for more than 6 months [32]. However, further study is needed to investigate the long-term properties of the NACP+QADM+NAg composite.

Besides antibacterial properties, the composite needs to possess load-bearing capability for tooth cavity restorations. The major challenges facing composite restorations are secondary caries and bulk fracture [16,17]. In this study, incorporating the QADM and NAg into the NACP composite did not significantly decrease the strength. The strengths of NACP +QADM, NACP+NAg, and NACP+QADM+NAg composites were similar to those of the two commercial composites. The elastic moduli of the antibacterial nanocomposites also matched those of the two commercial composites. This is likely because the nanocomposites contained not only NACP, but also 35% of glass particles for reinforcement. According to the manufacturers, CompositeF (Heliomolar) is indicated for Class I and II posterior restorations and Class III and IV anterior restorations, and CompositeNoF (Renamel) is indicated for Class III, IV, and V restorations. Therefore, the antibacterial NACP+QADM, NACP+NAg, and NACP+QADM+NAg composites with similar strength and elastic modulus may also be suitable for these applications. These new nanocomposites have two added benefits: the release of Ca and PO_4 ions for remineralization [45], and the antibacterial ability shown in this study. Further efforts are needed to optimize the design and processing of these types of nanocomposites, and to investigate systematically the physical, antibiofilm, and anti-caries properties.

5. Conclusions

QADM and NAg were incorporated into a calcium phosphate nanocomposite for the first time yielding a strong antibacterial activity. The new nanocomposites greatly reduced the CFU counts, metabolic activity, and lactic acid production of *S. mutans* biofilms, compared to two commercial composites. The mechanical properties of the nanocomposites matched those of the commercial composites. Adding QADM and NAg together in the NACP composite resulted in a significantly stronger antibacterial capability, than using QADM or NAg alone. Previous studies showed that the NACP nanocomposite released high levels of Ca and PO_4 ions that could remineralize tooth lesions. The novel NACP+QADM+NAg composite is promising to possess the double benefits of remineralization and antibacterial capabilities to inhibit dental caries.

Acknowledgments

We thank Dr. L. C. Chow and Dr. L. Sun of the American Dental Association Foundation (ADAF) for discussions, and Dr. Qianming Chen of the West China College of Stomatology for help. We are grateful to Esstech (Essington, PA) and Dr. Sibel A. Antonson at Ivoclar Vivadent (Amherst, NY) for donating the materials. We acknowledge the technical support of the Core Imaging Facility of the University of Maryland Baltimore. This study was supported by NIH R01 grants DE17974 and DE14190 (HX), NIDCR-NIST Interagency Agreement Y1-DE-7005-01, University of Maryland Dental School, NIST, and West China College of Stomatology.

References

[1]. Mjör IA, Moorhead JE, Dahl JE. Reasons for replacement of restorations in permanent teeth in general dental practice. International Dent J. 2000; 50:361–366.

[2]. Deligeorgi V, Mjor IA, Wilson NH. An overview of reasons for the placement and replacement of restorations. Prim Dent Care. 2001; 8:5–11. [PubMed: 11405031]

[3]. Frost PM. An audit on the placement and replacement of restorations in a general dental practice. Prim Dent Care. 2002; 9:31–36. [PubMed: 11901789]

[4]. NIDCR (National Institute of Dental and Craniofacial Research) announcement # 13-DE-102, Dental Resin Composites and Caries. March 5. 2009

[5]. Ferracane JL. Current trends in dental composites. Crit Rev Oral Biol Med. 1995; 6:302–318. [PubMed: 8664421]

[6]. Bayne SC, Thompson JY, Swift EJ Jr. Stamatiades P, Wilkerson M. A characterization of first-generation flowable composites. J Am Dent Assoc. 1998; 129:567–577. [PubMed: 9601169]

[7]. Lim BS, Ferracane JL, Sakaguchi RL, Condon JR. Reduction of polymerization contraction stress for dental composites by two-step light-activation. Dent Mater. 2002; 18:436–444. [PubMed: 12098572]

[8]. Watts DC, Marouf AS, Al-Hindi AM. Photo-polymerization shrinkage-stress kinetics in resin-composites: methods development. Dent Mater. 2003; 19:1–11. [PubMed: 12498890]

[9]. Lu H, Stansbury JW, Bowman CN. Impact of curing protocol on conversion and shrinkage stress. J Dent Res. 2005; 84:822–826. [PubMed: 16109991]

[10]. Xu X, Ling L, Wang R, Burgess JO. Formation and characterization of a novel fluoride-releasing dental composite. Dent Mater. 2006; 22:1014–1023. [PubMed: 16378636]

[11]. Drummond JL. Degradation, fatigue, and failure of resin dental composite materials. J Dent Res. 2008; 87:710–719. [PubMed: 18650540]

[12]. Svanberg M, Mjör IA, Ørstavik D. Mutans streptococci in plaque from margins of amalgam, composite, and glass-ionomer restorations. J Dent Res. 1990; 69:861–864. [PubMed: 2109000]

[13]. Imazato S, Torii M, Tsuchitani Y, McCabe JF, Russell RRB. Incorporation of bacterial inhibitor into resin composite. J Dent Res. 1994; 73:1437–1443. [PubMed: 8083440]

[14]. Zalkind MM, Keisar O, Ever-Hadani P, Grinberg R, Sela MN. Accumulation of Streptococcus mutans on light-cured composites and amalgam: An *in vitro* study. J Esthet Dent. 1998; 10:187–190. [PubMed: 9893513]

[15]. Beyth N, Domb AJ, Weiss E. An *in vitro* quantitative antibacterial analysis of amalgam and composite resins. J Dent. 2007; 35:201–206. [PubMed: 16996674]

[16]. Sakaguchi RL. Review of the current status and challenges for dental posterior restorative composites: clinical, chemistry, and physical behavior considerations. Dent Mater. 2005; 21:3–6. [PubMed: 15680996]

[17]. Sarrett DC. Clinical challenges and the relevance of materials testing for posterior composite restorations. Dent Mater. 2005; 21:9–20. [PubMed: 15680997]

[18]. Jokstad A, Bayne S, Blunck U, Tyas M, Wilson N. Quality of dental restorations. FDI Commision Projects 2–95. International Dent J. 2001; 51:117–158.

[19]. Loesche WJ. Role of *Streptococcus mutans* in human dental decay. Microbiological Reviews. 1986; 50:353–380. [PubMed: 3540569]

[20]. Featherstone JDB. The science and practice of caries prevention. J Am Dent Assoc. 2000; 131:887–899. [PubMed: 10916327]

[21]. Deng DM, ten Cate JM. Demineralization of dentin by *Streptococcus mutans* biofilms grown in the constant depth film fermentor. Caries Res. 2004; 38:54–61. [PubMed: 14684978]

[22]. Totiam P, Gonzalez-Cabezas C, Fontana MR, Zero DT. A new *in vitro* model to study the relationship of gap size and secondary caries. Caries Res. 2007; 41:467–473. [PubMed: 17827964]

[23]. Cenci MS, Pereira-Cenci T, Cury JA, ten Cate JM. Relationship between gap size and dentine secondary caries formation assessed in a microcosm biofilm model. Caries Res. 2009; 43:97–102. [PubMed: 19321986]

[24]. Imazato S. Review: Antibacterial properties of resin composites and dentin bonding systems. Dent Mater. 2003; 19:449–457. [PubMed: 12837391]

[25]. Imazato S. Bioactive restorative materials with antibacterial effects: new dimension of innovation in restorative dentistry. Dent Mater J. 2009; 28:11–19. [PubMed: 19280964]

[26]. Li F, Chen J, Chai Z, Zhang L, Xiao Y, Fang M, Ma S. Effects of a dental adhesive incorporating antibacterial monomer on the growth, adherence and membrane integrity of Streptococcus mutans. J Dent. 2009; 37:289–296. [PubMed: 19185408]

[27]. Xie D, Weng Y, Guo X, Zhao J, Gregory RL, Zheng C. Preparation and evaluation of a novel glass-ionomer cement with antibacterial functions. Dent Mater. 2011; 27:487–496. [PubMed: 21388668]

[28]. Tezvergil-Mutluay A, Agee KA, Uchiyama T, Imazato S, Mutluay MM, Cadenaro M, Breschi L, Nishitani Y, Tay FR, Pashley DH. The inhibitory effects of quaternary ammonium methacrylates on soluble and matrix-bound MMPs. J Dent Res. 2011; 90:535–540. [PubMed: 21212315]

[29]. Kourai H, Yabuhara T, Sjirai A, Maeda T, Nagamune H. Syntheses and antimicrobial activities of a series of new bis-quaternary ammonium compounds. Eur J Med Chem. 2006; 41:437–444. [PubMed: 16517025]

[30]. Thome T, Mayer MPA, Imazato S, Geraldo-Martins VR, Marques MM. *In vitro* analysis of inhibitory effects of the antibacterial monomer MDPB-containing restorations on the progression of secondary root caries. J Dent. 2009; 37:705–711. [PubMed: 19540033]

[31]. Antonucci JM, Fowler BO, Zeiger DN, Lin NJ, Lin-Gibson S. Synthesis and characterization of dimethacrylates containing quaternary ammonium functionalities for dental applications. Dent Mater. 2011 in review.

[32]. Yoshida K, Tanagawa M, Atsuta M. Characterization and inhibitory effect of antibacterial dental resin composites incorporating silver-supported materials. J Biomed Mater Res. 1999; 4:516–522. [PubMed: 10497286]

[33]. Tanagawa M, Yoshida K, Matsumoto S, Yamada T, Atsuta M. Inhibitory effect of antibacterial resin composite against *Streptococcus mutans*. Caries Res. 1999; 33:366–371. [PubMed: 10460960]

[34]. Monteiro DR, Gorup LF, Takamiya AS, Ruvollo-Filho AC, de Camargo ER, Barbosa DB. The growing importance of materials that prevent microbial adhesion: antimicrobial effect of medical devices containing silver. Int J Antimicrob Agent. 2009; 34:103–110.

[35]. Allaker RP. The use of nanoparticles to control oral biofilm formation. J Dent Res. 2010; 89:1175–1186. [PubMed: 20739694]

[36]. Morones JR, Elechiguerra JL, Camacho A, Holt K, Kouri JB, Ramirez JT, Yacaman MJ. The bactericidal effect of silver nanoparticles. Nanotechnology. 2005; 16:2346–53. [PubMed: 20818017]

[37]. Fan C, Chu L, Rawls HR, Norling BK, Cardenas HL, Whang K. Development of an antimicrobial resin - A pilot study. Dent Mater. 2011; 27:322–328. [PubMed: 21112619]

[38]. Cheng YJ, Zeiger DN, Howarter JA, Zhang X, Lin NJ, Antonucci JM, Lin-Gibson S. *In situ* formation of silver nanoparticles in photocrosslinking polymers. J Biomed Mater Res B. 2011; 97:124–131.

[39]. Skrtic D, Antonucci JM, Eanes ED, Eichmiller FC, Schumacher GE. Physiological evaluation of bioactive polymeric composites based on hybrid amorphous calcium phosphates. J Biomed Mater Res B. 2000; 53:381–391.

[40]. Dickens SH, Flaim GM, Takagi S. Mechanical properties and biochemical activity of remineralizing resin-based Ca-PO_4 cements. Dent Mater. 2003; 19:558–566. [PubMed: 12837405]

[41]. Xu HHK, Sun L, Weir MD, Antonucci JM, Takagi S, Chow LC. Nano dicalcium phosphate anhydrous-whisker composites with high strength and Ca and PO_4 release. J Dent Res. 2006; 85:722–727. [PubMed: 16861289]

[42]. Langhorst SE, O'Donnell JNR, Skrtic D. *In vitro* remineralization of enamel by polymeric amorphous calcium phosphate composite: Quantitative microradiographic study. Dent Mater. 2009; 25:884–891. [PubMed: 19215975]

[43]. Xu HHK, Weir MD, Sun L, Moreau JL, Takagi S, Chow LC, Antonucci JM. Strong nanocomposites with Ca, PO_4 and F release for caries inhibition. J Dent Res. 2010; 89:19–28. [PubMed: 19948941]

[44]. Chow LC, Sun L, Hockey B. Properties of nanostructured hydroxyapatite prepared by a spray drying technique. J Res NIST. 2004; 109:543–551.

[45]. Xu HHK, Moreau JL, Sun L, Chow LC. Nanocomposite containing amorphous calcium phosphate nanoparticles for caries inhibition. Dent Mater. 2011; 27:762–769. [PubMed: 21514655]

[46]. Lee Y, Lu H, Oguri M, Powers JM. Changes in gloss after simulated generalized wear of composite resins. J Prosthet Dent. 2005; 94:370–376. [PubMed: 16198175]

[47]. Cheng L, Weir MD, Xu HHK, Kraigsley AM, Lin N, Lin-Gibson S, Zhou X. Antibacterial and physical properties of calcium-phosphate and calcium-fluoride nanocomposites with chlorhexidine. J Biomed Mater Res B. 2011 in review.

[48]. Kraigsley AM, Lin-Gibson S, Lin NJ. Effects of polymer degree of conversion on oral biofilm metabolic activity and biomass. Biomaterials. 2011 in review.

[49]. van Loveren C, Buijs JF, ten Cate JM. The effect of triclosan toothpaste on enamel demineralization in a bacterial demineralization model. J Antimicrob Chemo. 2000; 45:153–158.

[50]. Stoodley P, Wefel J, Gieseke A, deBeer D, von Ohle C. Biofilm plaque and hydrodynamic effects on mass transfer, fluoride delivery and caries. J Am Dent Assoc. 2008; 139:1182–1190. [PubMed: 18762628]

[51]. Deng DM, van Loveren C, ten Cate JM. Caries-preventive agents induce remineralization of dentin in a biofilm model. Caries Res. 2005; 39:216–223. [PubMed: 15914984]

[52]. Moreau JL, Sun L, Chow LC, Xu HHK. Mechanical and acid neutralizing properties and inhibition of bacterial growth of amorphous calcium phosphate dental nanocomposite. J Biomed Mater Res Part B. 2011 accepted for publication.

[53]. Lee SB, Koepsel RR, Morley SW, Matyjaszewski K, Sun Y, Russell AJ. Permanent, nonleaching antibacterial surface. 1. Synthesis by atom transfer radical polymerization. Biomacromolecules. 2004; 5:877–882. [PubMed: 15132676]

[54]. Beyth N, Yudovin-Farber I, Bahir R, Domb AJ, Weiss EI. Antibacterial activity of dental composites containing quaternary ammonium polyethylenimine nanoparticles against Streptococcus mutans. Biomaterials. 2006; 27:3995–4002. [PubMed: 16564083]

[55]. Namba N, Yoshida Y, Nagaoka N, Takashima S, Matsuura-Yoshimoto K, Maeda H, Van Meerbeek B, Suzuki K, Takashida S. Antibacterial effect of bactericide immobilized in resin matrix. Dent Mater. 2009; 25:424–430. [PubMed: 19019421]

[56]. Li P, Li J, Wu C, Wu Q, Li J. Synergistic antibacterial effects of β-lactam antibiotic combined with silver nanoparticles. Nanotechnology. 2005; 16:1912–1917.

[57]. Slenters TV, Hauser-Gerspach I, Daniels AU, Fromm KM. Silver coordination compounds as light-stable, nano-structured and anti-bacterial coatings for dental implant and restorative materials. J Mater Chem. 2008; 18:5359–5362.

[58]. Rai M, Yada A, Gade A. Silver nanoparticles as a new generation of antimicrobials. Biotechnol Adv. 2009; 27:76–83. [PubMed: 18854209]

[59]. Damm C, Munsted H, Rosch A. Long-term antimicrobial polyamide 6/silver nanocomposites. J Mater Sci. 2007; 42:6067–6073.

[60]. Percival SL, Bowler PG, Russell D. Bacterial resistance to silver in wound care. J Hospital Infection. 2005; 60:1–7.

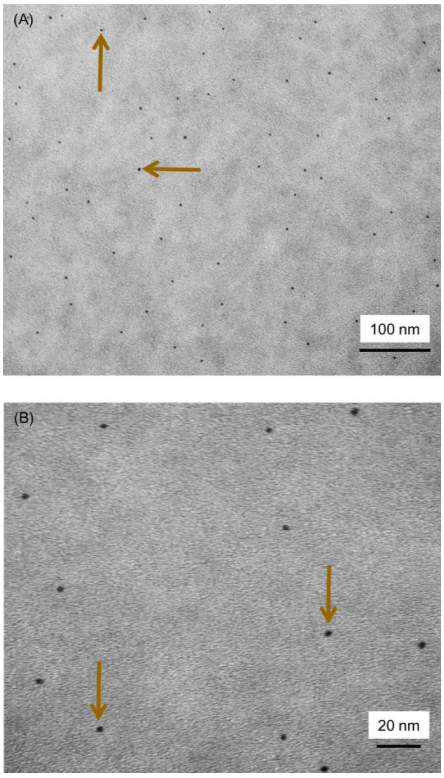

[1].
Representative TEM micrographs of the size and dispersion of silver nanoparticles in the resin matrix: (A) lower and (B) high magnification. Silver 2-ethylhexanoate salt was dissolved in 2-(tert-butylamino) ethyl methacrylate and incorporated into a BisGMA-TEGDMA resin at a silver salt mass fraction of 0.08% in the resin. The silver nanoparticles were formed in the resin by simultaneous reduction of the silver salt and photopolymerization of the dimethacrylates. The particle size was measured (mean ± sd; n = 100) to be (2.7 ± 0.6) nm. Arrows indicate the silver nanoparticles, which were well dispersed in the resin with minimal appearance of nanoparticle aggregates.

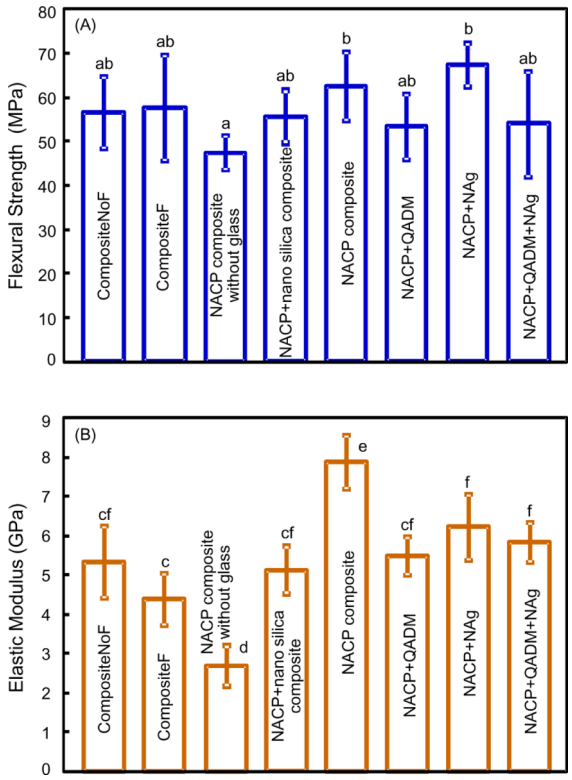

[2].

Mechanical properties. (A) Flexural strength, and (B) elastic modulus for CompositeNoF, CompositeF, NACP composite, NACP+QADM composite, NACP+NAg composite, and NACP+QADM+NAg composite. Each value is the mean of six measurements with the error bar indicating one standard deviation (mean ± sd; n = 6).

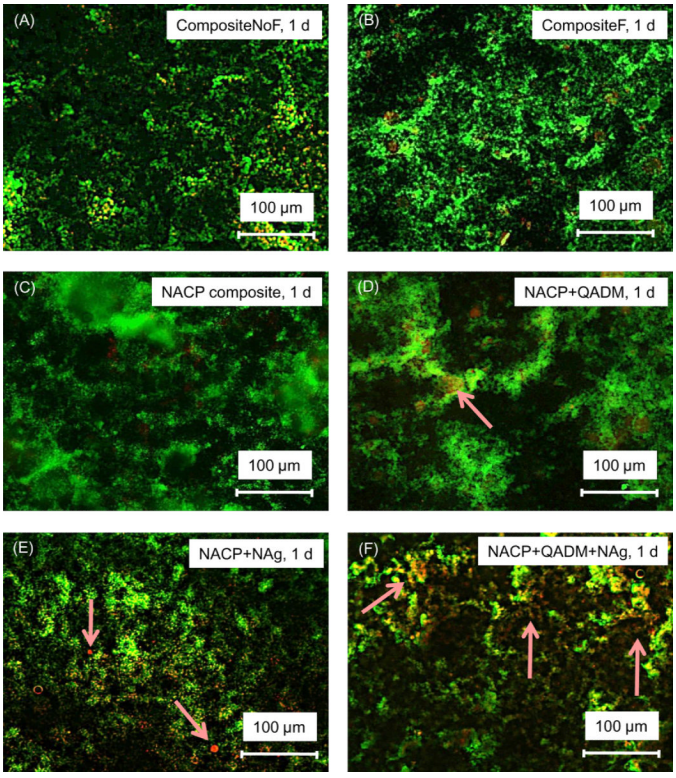

[3].

Live/dead fluorescence images of *S. mutans* biofilms on composites at 1 d: (A) CompositeNoF, (B) CompositeF, (C) NACP composite, (D) NACP+QADM composite, (E) NACP+NAg composite, (F) NACP+QADM+NAg composite. Live bacteria were stained green, and the compromised bacteria were stained red. When the live and dead bacteria were close to each other or on the top of each other, the green staining was mixed with the red, resulting in yellowish or orange colors. Arrows in D, E and F indicate areas of the compromised bacteria.

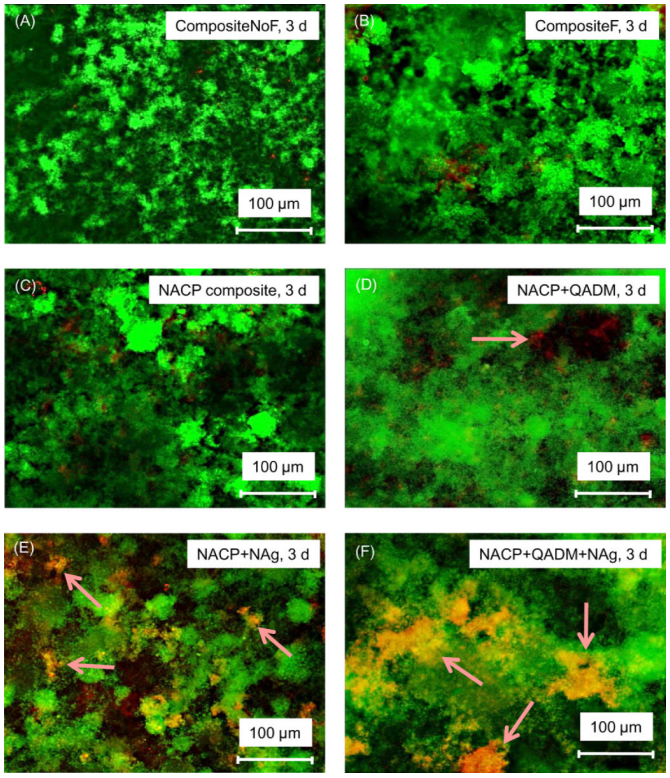

[4].

Live/dead fluorescence images of *S. mutans* biofilms on composites at 3 d: (A) CompositeNoF, (B) CompositeF, (C) NACP composite, (D) NACP+QADM composite, (E) NACP+NAg composite, (F) NACP+QADM+NAg composite. Arrows in D, E and F indicate areas of the compromised bacteria. A–C had mature biofilms in which the staining was mostly green, hence the bacteria were primarily alive. NACP+QADM+NAg composite had the most red/orange staining, indicating the greatest amount of compromised bacteria.

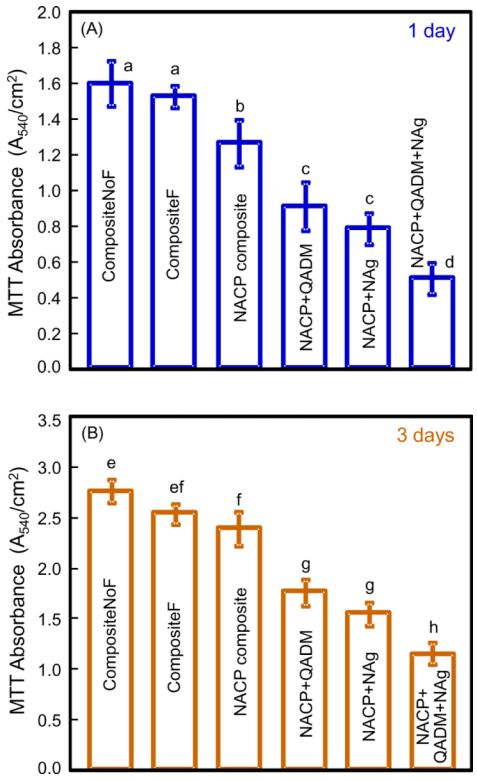

[5].

The metabolic activity of *S. mutans* biofilms adherent on CompositeNoF, CompositeF, NACP composite, NACP+QADM composite, NACP+NAg composite, and NACP+QADM +NAg composite. Metabolic activity was measured via the MTT assay at (A) 1 d, and (B) 3 d. In each plot, values (mean ± sd; n = 6) with dissimilar letters are significantly different ($p < 0.05$).

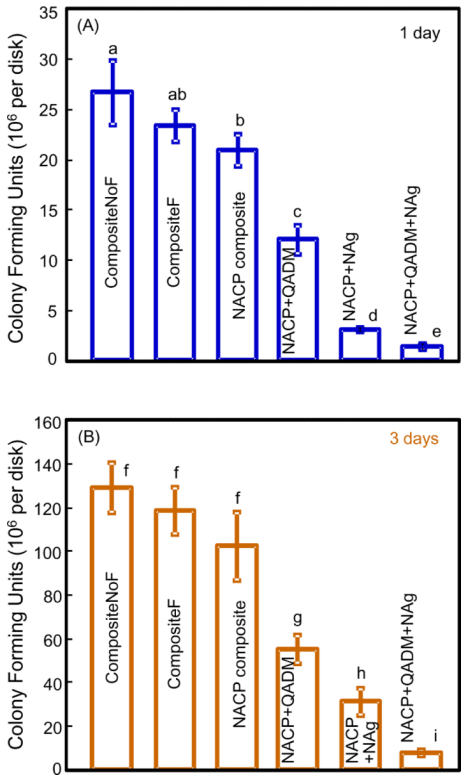

[6].

CFU counts of *S. mutans* biofilms adherent on the composites at (A) 1 d, and (B) 3 d, with the y-axis units being 10^6 bacteria per composite disk. In each plot, the values (mean ± sd; n = 6) indicated with dissimilar letters are significantly different from each other ($p < 0.05$). The NACP+QADM+NAg composite had the least CFU which was an order of magnitude less than that of CompositeNoF.

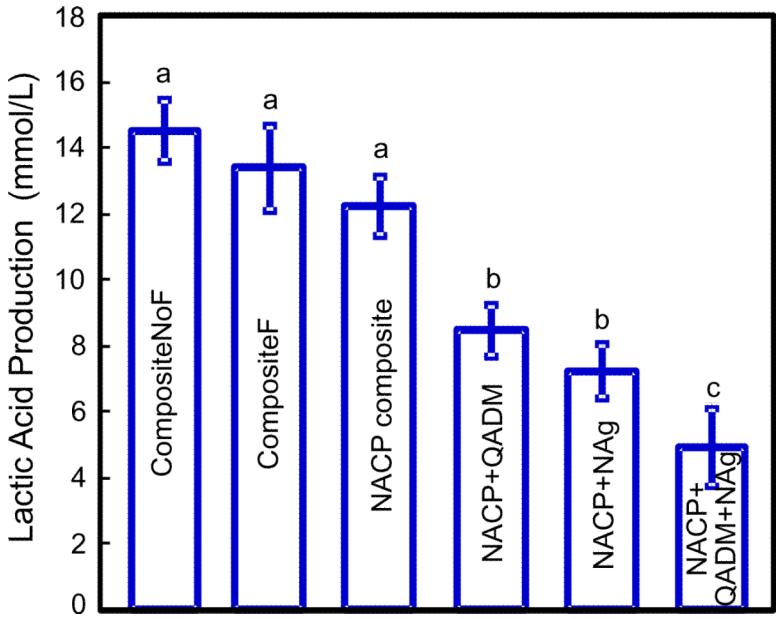

[7].

Lactic acid production by *S. mutans* biofilms adherent on disks of CompositeNoF, CompositeF, NACP composite, NACP+QADM composite, NACP+NAg composite, and NACP+QADM+NAg composite. Each value is mean ± sd; n = 6. Dissimilar letters indicate values that are significantly different from each other ($p < 0.05$).

Table 1

Compositions of Experimental Nanocomposites (% indicates mass fraction)*

	NACP	Glass	BisGMA-TEGDMA	QADM	NAg
NACP composite	30%	35%	35%	0%	0%
NACP+QADM composite	30%	35%	28%	7%	0%
NACP+NAg composite	30%	35%	34.972%	0%	0.028%
NACP+QADM+NAg composite	30%	35%	27.972%	7%	0.028%

* NACP refers to nanoparticles of amorphous calcium phosphate. Glass refers to barium boroaluminosilicate glass particles. BisGMA-TEGDMA refers to a BisGMA and TEGDMA mixture at 1:1 ratio plus 0.2% camphorquinone and 0.8% ethyl 4-N,N-dimethylaminobenzoate. NAg refers to nanoparticles of silver.